DOI: http://dx.doi.org/10.7551/978-0-262-31709-2-ch093



# Population dynamics with limited perception establish global swarm topology

Anna Shcherbacheva[1], Tuomo Kauranne[1]

[1]Lappeenranta University of Technology, Finland
anna.shcherbacheva@lut.fi
tuomo.kauranne@lut.fi



## Abstract

We simulate the swarming behavior of three synthetic animal species that differ only by the degree of perception they have on their fellow animals. The species are called *mosquitoes*, *birds* and *fish*. The swarms that comprise many individuals of each species in turn move randomly in a rugged potential landscape. The *mosquitoes* pay no heed to one another. The *birds* follow a bunch of their nearest neighbours in front, based on strictly limited visibility. The *fish*, in turn, sense also far-away neighbors through their lateral line, as modeled by an exponentially decaying perception function. The simulations show that such local differences in perception by swarming individuals have global macroscopic consequences to the geometry of the corresponding swarms. These consequences are of persistent nature across many simulations with each species.

## Introduction

Humans, like many other animal species, are social. We are fundamentally geared to living in a herd of some 20 - 100 individuals, from our nearest primate cousins to decide. Many other animal species have much more intense social lives, with flocks extending to thousands of individuals. Large flocks - or swarms - have their own requirements as to the means of imposing collective social control over the individuals involved. The process of social co-ordination is bi-directional: on the one hand, swarm dynamics exerts control over each individual. On the other, swarm dynamics is a direct consequence of the collective motion of all of its individuals.

In this article, we compare the consequences on collective dynamics of different degrees and forms of perception of swarming animals through computer simulations. Many studies indicate that the bi-directional flow of information described above has an important defining role in determining the nature of swarm dynamics. The impact of information flow boils down to the question of how do the individuals in a swarm perceive the collective dynamics of the swarm - and to the reciprocal question of how does the reaction of individuals influence the collective dynamics of the swarm.

We shall study this question with computer simulations of the collective motion of swarms of three different types of animals, all capable of moving in two spatial dimensions. These synthetic species are labeled as *mosquitoes*, *birds* and *fish*. They are set to move in a similar synthetic world with some external forces and constraints. But the way they perceive their fellow passengers is different, which has a fundamental impact on the nature of the corresponding collective motion of the swarm.

## Swarm dynamics with a difference

Collective swarm dynamics can be described in many ways, such as using ordinary or partial, deterministic or stochastic, differential equations. Classical models of *Eulerian type* (e.g., see Milewski and Yang (2008), Murray (2002), Mogilner and Edelstein-Keshet (1999) and Nagai and M. (1983)) are based on the **diffusion-advection-reaction** equation, governing the spatio-temporal dynamics of the population density:

$$\frac{\partial f}{\partial t} = \frac{\partial}{\partial x}\left(D(f)\frac{\partial f}{\partial x}\right) - \frac{\partial}{\partial x}\left(V(f)f\right) + B(f), \qquad (1)$$

where the first term on the right-hand side introduces a Brownian motion with diffusion coefficient $D(f)$, the second term stands for advection with density-dependent velocity $V(f)$ and the last reaction term may include birth or death processes.

Convection term results in attraction and repulsion effects, reflecting forms of social interaction between population members which implies that the direction and speed of motion of a particular individual is determined by the population density of the surrounding environment. One advantage of continuous models is the diversity of readily available analytic tools that facilitate their study.

Since the sensory systems of animals are limited, it is typically assumed that interactions have finite spatial influence. In most PDE-based models advection velocity is specified as a convolution (Mogilner and Edelstein-Keshet (1999),Edelstein-Keshet et al. (1997)):

$$V(f) = \mathbf{K} * f = \int_R \mathbf{K}(x - x')f(x', t)dx', \qquad (2)$$

where the kernel $K$ relates to the strength of animal-animal interaction per unit density with a distance $x - x'$ between two sites, see Mogilner and Edelstein-Keshet (1999).

Another common approach is based on modeling the movement of each individual member of the total population comprising $N$ identical members. In this so-called *Lagrangian approach* each individual member follows simple rules of motion, specified by either a system of stochastic differential equations, as was done in Burger et al. (2007), Morale et al. (2005), or via a hierarchical algorithm with a probabilistic decision-making mechanism, see Gueron et al. (1996).

In our simulations of synthetic animal swams, swarming *mosquitoes* do not affect each other. The main factor that determines their motion is sensing features of a potential prey or heat source. Host-seeking behavior of mosquitoes was thoroughly considered in Cummins et al. (2012). *Mosquitoes* were treated as a number of independent agents, sampling concentration of attractive odor emitted from host individuals via mechanism of **klinotaxis**. The concentration is given by the convection-diffusion equation. In the present study, the *mosquito* case is modeled with a similar approach, but by different means.

In order to focus our study on the influence of perception on collective dynamics, we use an identical environment for all the swarms. This environment consists of a two-dimensional landscape that resides at the bottom of a "potential bowl" that describes the local habitat of the swarm. The swarm is therefore confined to a limited, but boundaryless, area. Inside the potential bowl, there are four obstacles at the corners of a square that repel individuals and cause the swarm to turn away from them. These obstacles can represent e.g. trees, buildings, rocks or repellents.

The dynamics of a swarm are directed both by external forces - such as the potential bowl above that forms a basin of attraction, and the obstacles that each constitute a repulsive force - and by internal forces created by the autonomous dynamics generated by the members of the swarm through their interaction. Both external and internal forces are represented in population dynamics as force potentials that are mediated by perception. In our model, we assume the external forces to be constant in time and independent of swarm dynamics, so as to focus on the autonomous dynamics of the swarm. In the real world, both external and internal forces are very much dynamic, as can be seen e.g. from any movie of dolphins chasing a school of fish.

Our autonomous swarm dynamics are broadly following a class of stochastic differential equation models introduced by Capasso and Morale in Morale et al. (2005) and Burger et al. (2007). In this kind of dynamics, there is a long-range herding force that keeps the swarm together, and a short-range repulsion force that prevents individuals from colliding.

Our three fundamental species differ only in the way that they can perceive their fellow animals. All the three species are only synthetic forms of life, but they are each given a familiar name that links each synthetic species to a related animal species.

Figure 1: General layout: global attractive potential in the center and four local sources of repulsion.

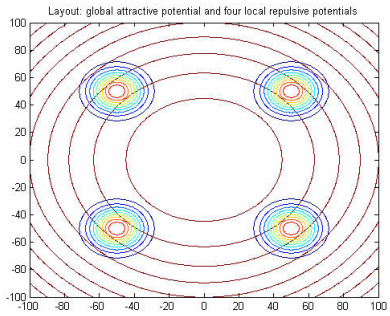


- *Mosquitoes* do not perceive their fellow mosquitoes. Instead they move in Brownian motion, weighted by the gradient of the external potential field alone.
- *Birds* do see their fellow birds, but only up to a fixed distance limit in their front.
- *Fish* may see only their immediate neighbors, but because of their special pressure sensing organ, the lateral line , they can feel the movement of the swarm beyond their range of visibility. In this case, their perception function is a radial, exponentially decaying function.

## Basic dynamic equations

We consider the general layout for the three above-mentioned cases, see Figure (1), where a source of global attractive potential is located at the center of the experimental habitat of the species, and four short-term repulsive potentials are placed separately from one another. In the case of a *mosquito* swarm, we treat this setting as an indoor space amended with four sources of repellent and one intensive heat source at the center. In the two other cases, the layout can be treated as a domain inhabited with a population of animals which contains four obstacles, such as trees or rocks.

### *Mosquito* swarm

The first case examines collective behavior of *mosquitoes* in presence of an intensive heat source and four patches covered with repellent (e.g., spray), modeled as a system of non-interacting particles driven by an external potential.

The heat source at $\mathbf{x}^h$ is modeled as a Gaussian hump:

$$C_a(\mathbf{x}) = exp\left[-\frac{d^2(\mathbf{x}, \mathbf{x}^h)}{2\sigma_a^2}\right], \qquad (3)$$

where $d(\mathbf{x}^h, \mathbf{x})$ is the distance between point $\mathbf{x}$ and the position of the source $\mathbf{x}^h$. The standard deviation of the Gaussian $\sigma_a$ conditions the minimal distance at which the *mosquito* is able to sense the heat.

We assume that each *mosquito* is driven towards the source by the mechanism of **klinotaxis**, as it was conjectured in Vickers (2000) for the case of host-seeking behavior of real mosquitoes. During klinotaxis, an animal samples the concentration of attractive substance at one location, then changes location and repeats sampling, using its memory of the concentration to choose its next position Cardé (1996).

In the present study, the klinotaxis mechanism is modeled by employing a random walk. The **Metropolis algorithm** was introduced in the 1950s in statistical physics literature as a tool to sample probability distributions, see Metropolis et al. (1953). The Metropolis algorithm is based on an **accept-reject** step. Assume that we take a step from point $\mathbf{x}^{n-1}$ to a candidate position $\mathbf{x}^n$. If corresponding probabilities are $p_{n-1}, p_n$, we accept the new position with probability

$$\alpha_a = min\left(1, \frac{p_n}{p_{n-1}}\right) \tag{4}$$

Hence, the upward steps ($p_n > p_{n-1}$) are always accepted, while steps downwards are accepted with probability $p_n/p_{n-1}$. Probabilities $p_n, p_{n-1}$ are taken from a **proposal distribution**. Applying the above-specified sampling rule with adequate proposal distribution implies that the samples converge towards the underlying target distribution.

In our simulations random walk is employed as a proposal distribution. Consider a *mosquito* at position $x_{n-1}$ at iteration $n-1$. It randomly selects a candidate position $\mathbf{x}^n$ by

$$\mathbf{x}^n = \mathbf{x}^{n-1} + \mathbf{dW}, \quad \mathbf{dW} \sim N(0, \mathbf{\Sigma}), \tag{5}$$

where the two-dimensional Gaussian $N(0, \mathbf{\Sigma})$ conditions the step length for the random walk. The probabilities are associated with the distribution of heat, and may be given as an exponential of the heat concentration: $p_n = exp(-C_a(\mathbf{x}^n)/2\sigma_a^2)$. The accept/reject probability can than be written as follows:

$$\alpha_a = \min\left(1, \tfrac{p_n}{p_{n-1}}\right) = \\ \min\left(1, exp\left[-(C_a(\mathbf{x}^{n-1}) - C_a(\mathbf{x}^n))/2\sigma^2\right]\right), \tag{6}$$

where $\sigma$ is a scale which governs the probability of a step away from the source to get accepted: the smaller is $\sigma$, the less likely they are to get accepted. Our *mosquito* 'sampler' is eventually supposed to roam in proximity to the heat source.

Repellent is treated as Heaviside step function which stands for a **probability of rejection** for candidate position $\mathbf{x}$:

$$\alpha_r(\mathbf{x}, \mathbf{x}^r) = \begin{cases} 1, & \min\limits_{j\in 1,\dots,N_r} d(\mathbf{x}, \mathbf{x}^r) \le L \\ 0, & \min\limits_{j\in 1,\dots,N_r} d(\mathbf{x}, \mathbf{x}^r) > L \end{cases}, \tag{7}$$

where $d(\mathbf{x}, \mathbf{x}^r)$ is a distance from position $\mathbf{x}$ to the source of repellent, $L$ determines the range of coverage. One way to combine multiple repellents is to sum rates of rejection over all sources of protection and take Metropolis-type of probability:

$$\alpha_r(\mathbf{x}^n) = \min(1, \sum_{i=1}^{N_r} \alpha_r(\mathbf{x}, \mathbf{x}_i^r)), \tag{8}$$

where $N_r$ is a total number of repellents. A *mosquito* swarm is represented as a number of individuals placed initially at random spatial positions on a rectangular patch $[x_{min}, x_{max}] \times [y_{min}, y_{max}]$. After that, every *mosquito* with initial position $\mathbf{x}^0$ changes its location in accordance with the following algorithm:

**Algorithm for swarm dynamics**

1. Select a candidate position $\mathbf{x}^n$ by adding Brownian increment to previous point, that is compute $\mathbf{x}^n$ by formula (5).
2. Measure concentration of heat at new position as it was specified in formula (3)
3. Compute **probability of acceptance** for position $\mathbf{x}^n$:

$$\alpha_a(\mathbf{x}^{n-1}, \mathbf{x}^n) = \\ \min \quad \left(1, exp\left[-(C_a(\mathbf{x}^{n-1}) - C_a(\mathbf{x}^n))/2\sigma^2\right]\right), \tag{9}$$

4. Compute **probability of rejection** by formula (8)
5. Generate a random number $r \sim U[0,1]$; if $r < \alpha_a(1 - \alpha_r)$, accept the new position $\mathbf{x}^n$. Otherwise, remain at the old position: $\mathbf{x}^n = \mathbf{x}^{n-1}$;
6. Move to step 1, $n \to n+1$.

## Flocks of *birds*

Our second type of swarming behavior also features dynamics under a global attractive potential. It can be viewed as a population moving inside a wide domain of habitation. This domain includes several areas covered with obstacles that are avoided by population members. External attraction and repulsion is treated as in the previous case of *mosquito* swarming behavior.

In contrast to *mosquitoes*, this second type of animals is supposed to coordinate with fellow-individuals, i.e. exhibit a tendency to aggregate but to avoid over-crowding. In our present simulations, both interactive effects are introduced by means of **Kalman dynamics**, a term derived from the statistical data assimilation method known as **The Kalman Filter**, see Kalman (1960), Evensen (2003).

The Kalman filter produces a **state estimate** of a dynamic system as a weighted average of a **prior state** or predicted state, and of a **state observation**.

Suppose that at the step $n-1$ *birds* have occupied positions

$$\mathbf{x}^{n-1} = \left(\mathbf{x}_1^{n-1}, \mathbf{x}_2^{n-1}, \ldots, \mathbf{x}_N^{n-1}\right), \tag{10}$$

where $N$ is the number of *birds*. Firstly, **prior candidate positions** $\mathbf{x}_i^n = \mathbf{x}_i^{n-1} + \mathbf{dW}, i = 1, \ldots, N$ are randomly selected and independent of one another. After that, every prior candidate point $\mathbf{x}_i^n, i = 1, \ldots, N$ is amended with an observational increment:

$$\overline{\mathbf{x}}_i^n = \mathbf{x}_i^n + G_a\left(\mathbf{y}_i^a - \mathbf{x}_i^n\right) \tag{11}$$

to introduce cohesion towards closest individuals, which is a typical way of attaining synchronization between animals, such as schooling fishes and flocking birds.

In the current case, we assume that a long-range attraction rule applies to the nearest five neighbors of each individual, as has been observed in the case of real birds. Positions of viewed fellow *birds* are combined into an artificial state observation

$$\mathbf{y}_i^a = \frac{1}{N_o}\sum_{j=j_1}^{j_{N_o}} \mathbf{x}_j^n, \tag{12}$$

where $j_a, \ldots, j_{N_o}$ are indeces of $N_o$ closest neighbors to the side and ahead of the agent $\mathbf{x}_i^n$.

The **Kalman Gain** $G_a$ can be adjusted to achieve a particular strength of cohesion: increasing $G_a$ implies enhancement of aggregative behavior.

Short-range repulsion between *birds* can be modeled similarly:

$$\overline{\mathbf{x}}_i^n = \mathbf{x}_i^n - G_r\left(\mathbf{y}_i^r - \mathbf{x}_i^n\right), \tag{13}$$

where observation $\mathbf{y}$ is composed as an average over the set $\mathcal{N}_r = \{j | d(\mathbf{x}_i^n \mathbf{x}_j^n) < d_{\min}\}$ of all positions located closer than at minimum distance $d_{\min}$:

$$\mathbf{y}_i^r = \frac{1}{|\mathcal{N}_r|}\sum_{j\in\mathcal{N}_r} \mathbf{x}_j^n. \tag{14}$$

Analogously to the above-described case of cohesion, the Kalman gain $G_r$ in formula (13) governs the strength of repulsive interaction.

**Algorithm for collective dynamics** is applied to each individual agent $i = 1, \ldots, N$ separately

1. Select a candidate position randomly:

$$\mathbf{x}_i^n = \mathbf{x}_i^{n-1} + \mathbf{dW}, \mathbf{dW} \sim N(0, \mathbf{\Sigma}). \tag{15}$$

2. Compute **probability of acceptance** for position $\mathbf{x}_i^n$:

$$\alpha_a = \min\left(1, e^{-\frac{(C_a(\mathbf{x}_i^{n-1}) - C_a(\mathbf{x}_i^n))}{2\sigma^2}}\right) \tag{16}$$

3. Compute **probability of rejection** for position $\mathbf{x}_i^n$:

$$\alpha_r = \begin{cases} 1, & \min\limits_{j\in 1,\ldots,N_r} d(\mathbf{x}_i^n, \mathbf{x}_j^r) \le L \\ 0, & \min\limits_{j\in 1,\ldots,N_r} d(\mathbf{x}_i^n, \mathbf{x}_j^r) > L \end{cases}, \tag{17}$$

where $d(\mathbf{x}_i^n, \mathbf{x}_j^r)$ is a distance between the $i$-th agent and the center of $j$-th obstruct patch, $L$ stands for the width of the patch,

4. Accept new position $\mathbf{x}_i^n$ with probability $\alpha_a(1-\alpha_r)$, in case of rejection, stay at the old position $\mathbf{x}_i^n = \mathbf{x}_i^{n-1}$,

5. Apply Kalman dynamics to induce interactive behavior (cohesion and repulsion):

$$\begin{aligned} \overline{\mathbf{x}}_i^n = \mathbf{x}_i^n \quad & + G_a\left(\mathbf{y}_i^a - \mathbf{x}_i^n\right) \\ & - G_r\left(\mathbf{y}_i^r - \mathbf{x}_i^n\right), \end{aligned} \tag{18}$$

where observations $\mathbf{y}_i^r$ and $\mathbf{y}_i^a$ are computed by formulas (12) and (14), correspondingly;

6. Compute probability of rejection $\alpha_r'$ for position $\overline{\mathbf{x}}_i^n$ by formula specified in the item 3, accept position ($\mathbf{x}_i^n = \overline{\mathbf{x}}_i^n$) with probability $1-\alpha_r'$, otherwise, remain at the old position $\mathbf{x}_i^n$,

7. Move to step 1, $n \to n+1$.

## Schools of *fish*

Schooling behavior is modeled similarly to the previous case, except for the observation stage for cohesion. *Fish* are characterized by their ability to sense their fellow kin even beyond a certain range, which is reflected in the perception function applied at the state observation step as follows:

$$\mathbf{y}_i^n = \sum_{\substack{j=1 \\ j\neq i}}^{N} \exp\left[-\lambda d(\mathbf{x}_i^n \mathbf{x}_j^n)\right] \mathbf{x}_j^n, \tag{19}$$

where observation weights decay exponentially with distance.

## Results

As to the pun in the title of the article - *mosquitoes* do not recognize any friends. *Mosquitoes*, by their definition as Markovian synthetic animals without regard for their fellow kin, keep happily flying on top of one another. It is lucky that they can be regarded as point-like particles in simulations!

The results of the simulations for all three species are illustrated in Figure 2. The three rows of the figure represent the three species. The columns from left to right represent an early state, one or two intermediate states, and a late state of the swarm, respectively, in each case. The upper-most left figure represents the common random initial state of all

Table 1: Values of model coefficients employed in experimental runs.

| parameters | values |
|---|---|
| $\sigma_a$ | 1000 |
| $L$ | 4 |
| $G_a$ | 0.7 |
| $G_r$ | 0.9 |
| $\lambda$ | 1 |
| $\sigma$ | $1e-3$ |

Figure 2: 1.Initial layout, 2.*Mosquito* swarm distribution at an intermediate stage, 3.The final distribution of the *mosquito* swarm, 4.-5. Intermediate distributions of *birds*, 6. The final distribution of *birds* ,7.-8. Intermediate distributions of *fish* , 9. The final distribution of *fish*

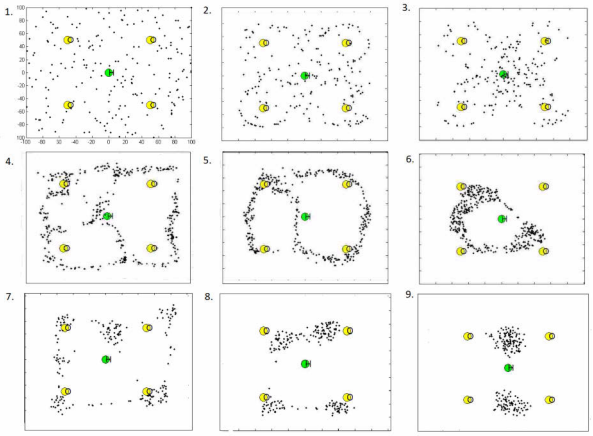

three swarms. From these figures, we conclude that the answer to the pun is not the same for *birds* and *fish* as it is for *mosquitoes*. The former two species both react to their fellow flyers or swimmers, in a manner that has a fundamental impact on the geometry of the swarms they form. Despite the slightly different forms of the algorithms used for *mosquitoes* and for the other two "species" of synthetic creatures, their swarms start out similar. The disregard for fellow *mosquitoes* causes them to get distributed according to the geometry of the landscape, but concentrating on the level contours of their potential well. Only in late stages of the simulation do *mosquitoes* finally find their way to the bottom of their potential bowl.

*Birds*, on the other hand, are so attached to their fellow fliers that this property actually prevents them from reaching the bottom of the potential bowl. Instead, they circulate in a simply or multiply connected chain to the foreseeable future. This is caused by the attractive potential of the nearest *birds* that inexorably pull the *birds* away from their preferred feeding ground, because of the "horror vacui" that surrounds it.

Finally, *fish* display yet another variety of swarm dynamics, since they can sense the presence of also far-away fellow swimmers. This property allows them to cluster into groups, instead of a continuous chain. In our rugged landscape, the end result is not a single cluster, but two clusters of *fish*, held away from each other and from the best feeding ground by the balance of mutual repulsion that would strengthen if the two schools would move closer to one another.

In all three cases, the final distributions of the swarms, flocks and schools are quite stable over many cycles of simulations. They therefore demonstrate clearly the macroscopic geometric consequences of the local degree of perception attributed to each synthetic species.
Increasing Kalman gain $G_a$ induces clustering behavior in the swarm, hence the latter parameter should be kept sufficiently big to stimulate cohesion, but not exceedingly large, since it annihilates the motion caused by an external potential. To avoid this effect, Kalman gain which governs the attraction should be smaller than matching repulsion coefficient $G_r$, see Table (1).

## Discussion

We have demonstrated that under similar but non-homogeneous geometric circumstances, the degree of local perception by swarming animals has global geometric consequences for their corresponding swarm dynamics. Instead of behaving in a totally random or chaotic fashion, the swarms adopt persistent geometric shapes that are a function of the degree of local perception possessed by the individuals in the swarm, even as the individuals generally move in a similar stochastic manner. We have demonstrated three such geometries in the case of three synthetic species that behave like mosquitoes, birds and fish, respectively.

This empirical result is not very surprising, in view of corresponding results in deterministic differential geometry. In differential geometry, the difference between the dimensions of the kernel and co-kernel and of a local linear curvature operator, such as the Laplacian, determines uniquely the Euler characteristic of the manifold, as is stated by the Atiyah-Singer Index Theorem and its many analogues and generalizations. The Euler characteristic describes the difference between the number of edges and the number of vertices of an arbitrary triangulation, or simplicial complexification in dimensions higher than two, of the corresponding manifold and it is a topological invariant. This means that the Euler characteristic remains the same, no matter how the triangulation or simplicial complex have been constructed. It is, in particular, independent of the lenght of the edges in such a triangulation, and hence on its spatial resolution.

On the other hand, there are well-known analogies between curvature operators and random walks, such as the bijective relationship between Brownian motion and the

Laplacian. It is not trivial to extend such results, that depend crucially on the linearity of the curvature operator, to the non-linear stochastic dynamics discussed in the current paper. But the persistence of the limit geometry of the swarms observed in our numerical experiments seems to indicate that the bridge of analogies from random walks through corresponding differential dynamics onto the global topology of the limit swarm on a non-trivially connected manifold is a continuous path. But the fact that the resulting topology is different for different perception operators testifies to the non-trivial nature of these analogies: the topology of the swarm is not uniquely determined by the topology of the underlying spatial manifold, but also depends on the non-linear perception operator associated with the swarm dynamics.

## References


Burger, M., Capasso, V., and Morale, D. (2007). On an aggregation model with long and short range interactions. *Nonlinear Analysis: Real World Applications*, 3:939–958.

Cardé, R. (1996). Odour plumes and odour-mediate flight in insects. In *Olfaction in mosquito-host interactions.*, number 200 in Ciba Foundation Symposium, page 54–66. John Wiley and Sons Ltd.

Cummins, B., Cortez, R., Foppa, I., Walbeck, J., and Hyman, J. (2012). A spatial model of mosquito host-seeking behavior. *PLoS Comput Biol*, 8(2):e1002500.

Edelstein-Keshet, L., Watmough, J., and Gr´unbaum, D. (1997). Do travelling band solutions describe cohesive swarms? an investigation for migratory locusts. *Journal of Mathematical Biology*, 36:515–549.

Evensen, G. (2003). The ensemble kalman filter: theoretical formulation and practical implementation. *Ocean Dynamics*, 53:343–367.

Gueron, S., Levin, S., and Rubenstein, D. (1996). The dynamics of herds: from individuals to aggregations. *Juornal of Theoretical Biology*, 182:85–98.

Kalman, R. E. (1960). A new approach to linear filtering and prediction problems. *Transactions of the ASME–Journal of Basic Engineering*, 82(Series D):35–45.

Metropolis, N., Rosenbluth, A., Rosenbluth, M., Teller, A., and Teller, E. (1953). Equations of state calculations by fast computing machines. *Journal of Chemical Physics*, 21(6):1087–1092.

Milewski, P. A. and Yang, X. (2008). A simple model for biological aggregation with asymmetric sensing. *Communications in Mathematical Sciences*, 6(2):397–416.

Mogilner, A. and Edelstein-Keshet, L. (1999). A non-local model for a swarm. *Journal of Mathematical Biology*, 38:534–570.

Morale, D., Capasso, V., and Oelschläger, K. (2005). An interacting particle system modelling aggregation behavior: from individuals to populations. *Journal of Mathematical Biology*, 50(1):49–66.

Murray, J. (2002). *Mathematical Biology I. An Introduction*. Springer.

Nagai, T. and M., M. (1983). Some nonlinear degenerate diffusion equations related to population dynamics. *The Journal of the Mathematical Society of Japan*, 35:539–561.

Vickers, N. (2000). Mechanisms of animal navigation in odor plumes. *Biological Bulletin*, 198:203–212.